Stress, Sheet Resistance, and Microstructure Evolution of Electroplated Cu Films During Self-Annealing

Rui Huang, Werner Robl, Hajdin Ceric, Thomas Detzel, and Gerhard Dehm

***Abstract*—Electroplated copper films are known to change their microstructure due to the self-annealing effect. The self-annealing effect of electroplated copper films was investigated by measuring the time dependence of the film stress and sheet resistance for different layer thicknesses between 1.5 and 20 μm. While the sheet resistance was found to decrease as time elapsed, a size-dependent change in film stress was observed. Films with the thickness of 5 μm and below decrease in stress, while thicker films initially reveal an increase in film stress followed by a stress relaxation at a later stage. This behavior is explained by the superposition of grain growth and grain-size-dependent yielding.**

***Index Terms*—Copper, film stress, microstructure, self-annealing, sheet resistance.**

I. Introduction

Copper has frequently replaced aluminum for interconnect applications in semiconductor devices due to its higher electrical conductivity, increased electromigration resistance, and better thermal conductivity [1], [2]. Electrochemical deposition (ECD) of copper has been demonstrated as one of the best methods to be adopted for high-performance logic devices using dual damascene technology and for power devices using pattern plating technology [3]–[5]. The recrystallization of ECD Cu at room temperature, which is termed self-annealing, is a very distinct phenomenon [6]–[10]. Microstructure evolution occurs during a transient period of hours following deposition and includes an increase in grain size, a change in film stress, and a decrease in sheet resistance. The self-annealing impacts subsequent processing steps, may require expensive postdeposition treatments, and can cause reliability impairment. A fundamental understanding of the self-annealing phenomenon is of great scientific and technological importance in order to ensure the stability of electrodeposited Cu metallization.

So far, most of the research has been devoted to ECD Cu films with thicknesses ranging from several hundreds of nanometers up to about 2 μm [6], [8], [9], [11]–[19] but was recently extended to studies on 70-μm-thick ECD Cu films [20], [21]. In these studies, grain growth was observed during room temperature annealing, accompanied by a continuous relaxation of film stress and sheet resistance [8], [9], [18], [19]. The grain growth is believed to be either induced by the initial high dislocation density triggering recrystallization or by surface segregation of impurities releasing the pinned grain boundaries [9], [13], [14], [22]. If the stress is initially compressive [9], [23], grain growth and annealing of defects will cause a reduction of the stress. However, for films which are initially under tensile stress after deposition [8], [12], [18], [19], grain growth would increase the tensile stress and therefore cannot explain a stress decrease. In such cases, other mechanisms must be active, which will be discussed in this paper.

In this paper, we focused our attention on the onset of stress relaxation for the film-thickness range of 1.5–20 μm which has not been investigated yet to the best of our knowledge. In this thickness regime, the grain size should span from ∼50 nm directly after deposition to the dimensions which are finally comparable to the film thickness after the grain growth. For this change in grain size, a strong size effect in plasticity should exist which may shed new insights in the self-annealing phenomenon of ECD Cu films. In addition, the investigated thickness range of the ECD Cu films covers the relevant thickness in power devices with their high demand on current capacity and heat dissipation [24].

Manuscript received April 26, 2009; revised July 14, 2009. First published September 22, 2009; current version published March 5, 2010. This work was supported in part by the Federal Ministry of Economics and Labor of the Republic of Austria under Contract 98.362/0112-C1/10/2005 and in part by the Carinthian Economic Promotion Fund (KWF) under Contract 18911, 13628, 19100.

R. Huang is with Kompetenzzentrum Automobil- und Industrieelektronik (KAI) GmbH, 9500 Villach, Austria, and also with the Institute for Microelectronics, Technische Universität Wien, 1040 Vienna, Austria (e-mail: rui.huang@k-ai.at).

W. Robl is with Infineon Technologies AG, 93049 Regensburg, Germany.

H. Ceric is with the Institute for Microelectronics, Technische Universität Wien, 1040 Vienna, Austria.

T. Detzel is with Infineon Technologies Austria AG, 9500 Villach, Austria.

G. Dehm is with the Department of Materials Physics, Montanuniversität Leoben, 8700 Leoben, Austria, and also with the Erich Schmid Institute of Material Science, Austrian Academy of Sciences, 8700 Leoben, Austria.

Color versions of one or more of the figures in this paper are available online at http://ieeexplore.ieee.org.

Digital Object Identifier 10.1109/TDMR.2009.2032768

II. Experimental Procedure

All investigated Cu films were prepared by electrochemical deposition on 8-in (∼200-mm) blanket wafers. Prior to the electrochemical deposition, a 100-nm-thick thermal oxide was deposited by chemical vapor deposition on the wafers as an isolation layer. Subsequently, a 50-nm-thick Ti film was deposited as an adhesion layer and diffusion barrier, followed by a 150-nm-thick Cu sputter-deposited seed layer. The barrier and seed layers were deposited in the same sputter tool without breaking the vacuum. The plating process was performed with a commercial fountain plating system. The electrolyte solution was mainly composed of Cu_2SO_4, H_2SO_4, and HCl, and with

1530-4388/$26.00 © 2010 IEEE

Authorized licensed use limited to: Universitatsbibliothek der TU Wien. Downloaded on April 26,2010 at 13:49:58 UTC from IEEE Xplore. Restrictions apply.

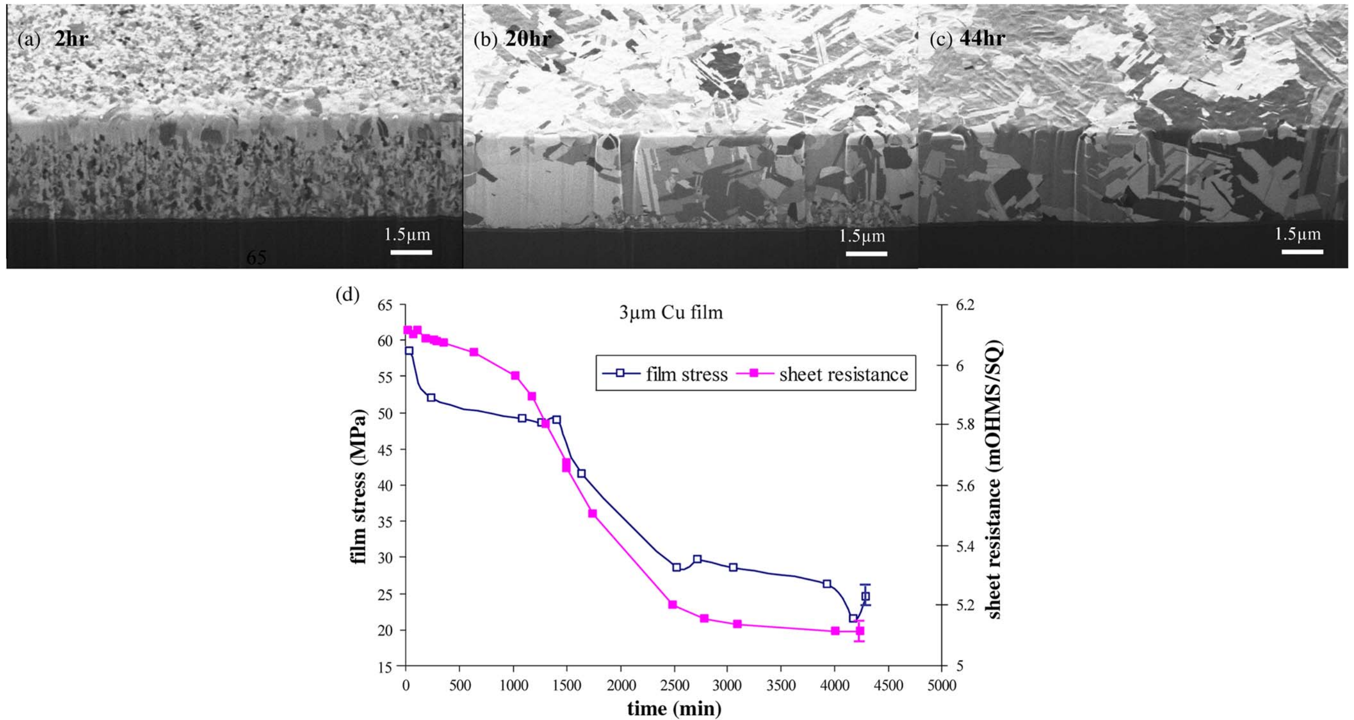

Fig. 1. (a), (b), and (c) Microstructure evolution of a 3-μm-thick Cu film, imaged with FIB using secondary electrons. A cross section has been cut in the film, which is imaged at a tilt angle of 45°, in order to resolve the surface and cross section. Note that the coarse grains which have formed at the intersection of the film surface and cross section in (a) are due to the FIB ion bombardment, which locally provides energy for grain growth. These grains were neglected when calculating the mean grain size. (d) Sheet resistance and film stress decrease during room-temperature annealing within ~50 h and subsequently saturate up to ~70 h, where the measurement was terminated. The error bar of sheet resistance was determined by the standard deviation of the measurement. The average film stress was determined by the wafer curvature measurement. Each stress measurement was repeated five times, and the average value was shown in (d). The error bar of film stress is determined by the deviation percentage of each measurement value to the average value.

two organic additives, an accelerator, and a suppressor with leveling components. An ac–dc combination was applied [24]. The whole ECD process consecutively undergoes a prewet in methane sulfonic acid, Cu electroplating, and a water rinse followed by a spin-dry process. The plating rate was kept constant for all Cu thicknesses, so that the impact of deposition speed on film properties was avoided. Finally, a wide split plan of ECD Cu thickness was applied from 1.5 to 20 μm.

All blanket ECD Cu layers were characterized as a function of time at room temperature. Sheet-resistance measurements were started 15 min after deposition and repeated in short time intervals up to ~100 h in order to trace the onset and kinetics of self-annealing. It was remeasured after approximately four months to detect the saturation of sheet resistance. In our experiment, sheet resistance was measured by a four-point probe system (Omnimap) performing 49 points evenly distributed over the wafer surface. In order to determine the film stress, the wafer curvature was monitored by a capacitance probe setup (Eichhorn and Hausmann) starting 30 min after deposition up to ~100 h and remeasured after approximately four months to detect the saturation of film stress, based on which, film stress can be calculated by using Stoney's equation [25]–[27]

$$\sigma = \frac{Eh^2}{(1-v)6t}\left(\frac{1}{R_2} - \frac{1}{R_1}\right) \tag{1}$$

where σ is the film stress, E corresponds to the elastic modulus of the substrate, ν denotes the Poisson's ratio of the substrate, h and t are the thicknesses of the substrate and film, and R_1 and R_2 are the measured radii of curvature before and after the electrochemical deposition of Cu films, respectively. Thus, for all reported stresses of the ECD Cu film, contributions from the underlying thermal oxide layer as well as the Ti and Cu seed layers have been eliminated.

The microstructure evolution was investigated for 3-, 8-, and 20-μm-thick films 2, 20, and 44 h after deposition by focused ion beam (FIB) microscopy (Micrion 9500) with the aim to correlate the change in grain size with sheet resistance and film stress. The average grain size is calculated by a linear intercept method based on FIB images recorded at 10 K magnification. The grains on cross section from bottom to top excluding the extreme top ones at the edge were captured to estimate the grain size. Twins are counted as grains. Due to the resolution limit of FIB images, the minimum grain size that can be detected is ~50 nm. The 45° tilt angle of the FIB images has been taken into account for the grain-size analysis in this study.

III. RESULTS

The evolution of sheet resistance and film stress of 3-μm Cu films is shown in Fig. 1. Initially, the sheet resistance has an incubation period of ~500 min, after which, it starts to decay rapidly, and finally, it stagnates at a sheet-resistance value of 5.1 mΩ/sq after ~3000 min. Similarly, the film stress decreases continuously to a final value of ~24 MPa. In order to correlate microstructure changes with the evolution of sheet resistance and film stress, FIB images were taken. The first FIB image

Authorized licensed use limited to: Universitatsbibliothek der TU Wien. Downloaded on April 26,2010 at 13:49:58 UTC from IEEE Xplore. Restrictions apply.

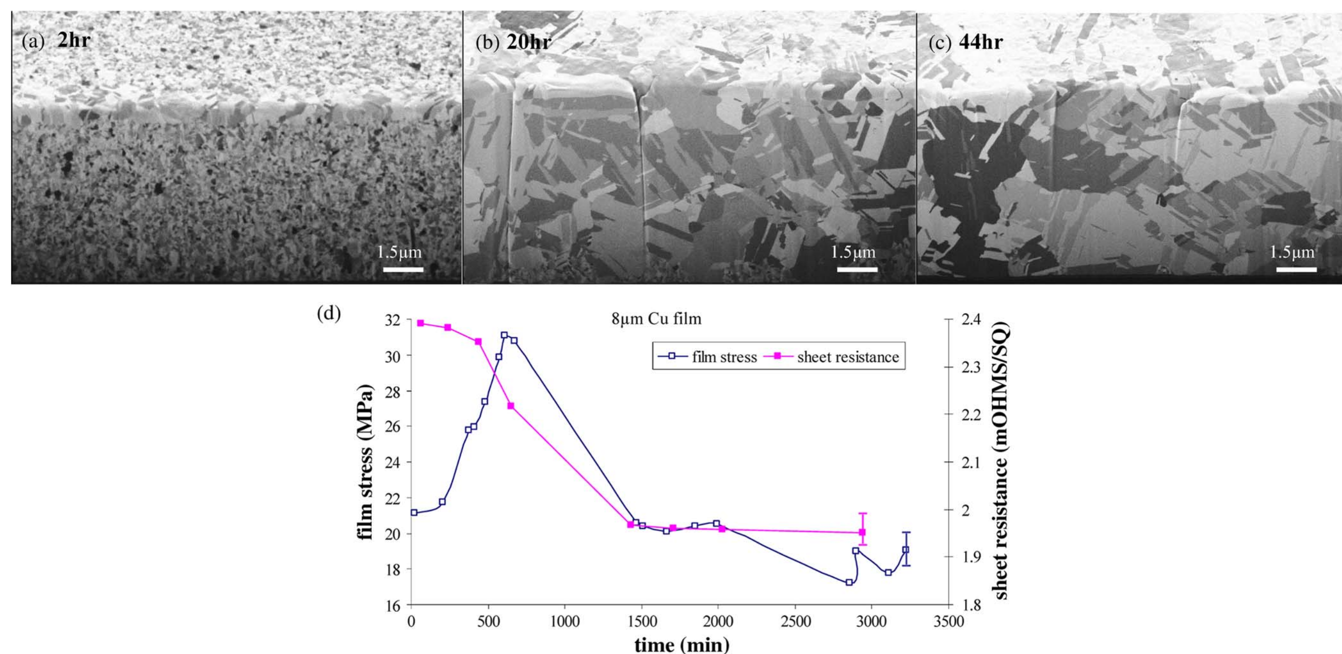

Fig. 2. (a), (b), and (c) Microstructure evolution of an 8-μm-thick Cu film. The cross section is imaged with a tilt angle of 45°. The coarse grains formed due to ion bombardment at the intersection of the film surface and cross section in (a) are neglected when grain size is calculated. (d) Sheet resistance decreases at room temperature as time elapses. The film stress increases until ∼12 h after deposition and then decreases. The error bars for sheet resistance and film stress are provided at the end of curves, respectively.

taken 2 h after deposition reveals a fine globular grain structure with an average grain size of ∼105 nm. After 20 h, a significant change in grain size has occurred. The grains which frequently contain twins now have a bimodal grain-size distribution with average grain sizes of either ∼190 or ∼1000 nm. Note that, at the Cu/substrate interface, a ∼300-nm-thick region of fine grains (∼105 nm in size) still exists. After 44 h, all fine grains have been consumed by large grains. Some of the grains (columnar grains) extend through the complete thickness but contain twins. The coexistence of columnar grains and twins leads again to a bimodal grain-size distribution of ∼220 and ∼1300 nm, exceeding the bimodal grain sizes after 20 h.

For 8- and 20-μm-thick Cu films, a similar effect as described for the 3-μm-thick Cu film has been observed for the sheet resistance and the grain evolution. However, their tendency of film-stress evolution is surprisingly different, as shown in Figs. 2 and 3. The film stress first increases within ∼600 min by ∼10 MPa and then decreases considerably until 1500 min to reach the stagnation for the 8-μm-thick Cu film. Different from that, the stress for the 20-μm-thick Cu film increases by 7 MPa in ∼600 min and then stagnates. There is no remarkable decrease of the stress observed. FIB images of the 8- and 20-μm-thick Cu films indicate, like in the case of the 3-μm-thick film (Fig. 1), that coarse grains form at the surface and then proceed toward the film/substrate interface, with large grains growing at the expense of smaller grains. Twins are visible in the large grains.

The results clearly indicate an influence of film thickness on the stress evolution. This becomes even more evident when comparing the stress–time evolution for film thickness ranging from 1.5 to 20 μm (Fig. 4). All films show tensile stress. Thin Cu films (1.5–5 μm) have relatively high initial stress (greater than ∼35 MPa) compared to thick Cu films (8–20 μm; less than ∼21 MPa). The evolution of film stress with time shows a disparate tendency between these two groups: 1) "thin" films with thickness of 5 μm and below and 2) "thick" films with the thickness of 8–20 μm. The tensile stress of thin films continues to decrease with time, while for thick Cu films, the stress first increases and, subsequently, after ∼700 min, begins to decrease or stagnate, depending on the maximum stress value. It is also worth to note that, within the first ∼200 min, 8–20-μm-thick ECD Cu films exhibit an incubation period, where the stress remains rather constant, while this is not observed for thin Cu films in this paper. Finally, the tensile stress values of all Cu films stagnate at a certain stress value, which is determined by the film thickness (grain size). Thicker films reveal a lower final stress after four months of relaxation than thinner films. Interestingly, the as-deposited film stress with its nanocrystalline microstructure shows also an inverse relationship between film stress and film thickness.

For the sheet-resistance change with time, three regions are observed, as shown in Fig. 5: I) Within the first ∼500 min, all Cu films irrespective of their thickness, exhibit a period of weakly decreasing sheet resistance, which is often referred in the literature as an incubation period [9], [14], [28]; II) a noticeable decrease of sheet resistance occurs, which is termed transient region; and III) a stagnation in sheet resistance is reached. This general behavior leads to a matching of normalized sheet resistance versus time curves for film thicknesses of 5 μm and larger, which results in a decay by ∼20%. In contrast to that, regions II and III are more sluggish for the 1.5- and 3-μm-thick films compared to 5-μm and thicker films.

Authorized licensed use limited to: Universitatsbibliothek der TU Wien. Downloaded on April 26,2010 at 13:49:58 UTC from IEEE Xplore. Restrictions apply.

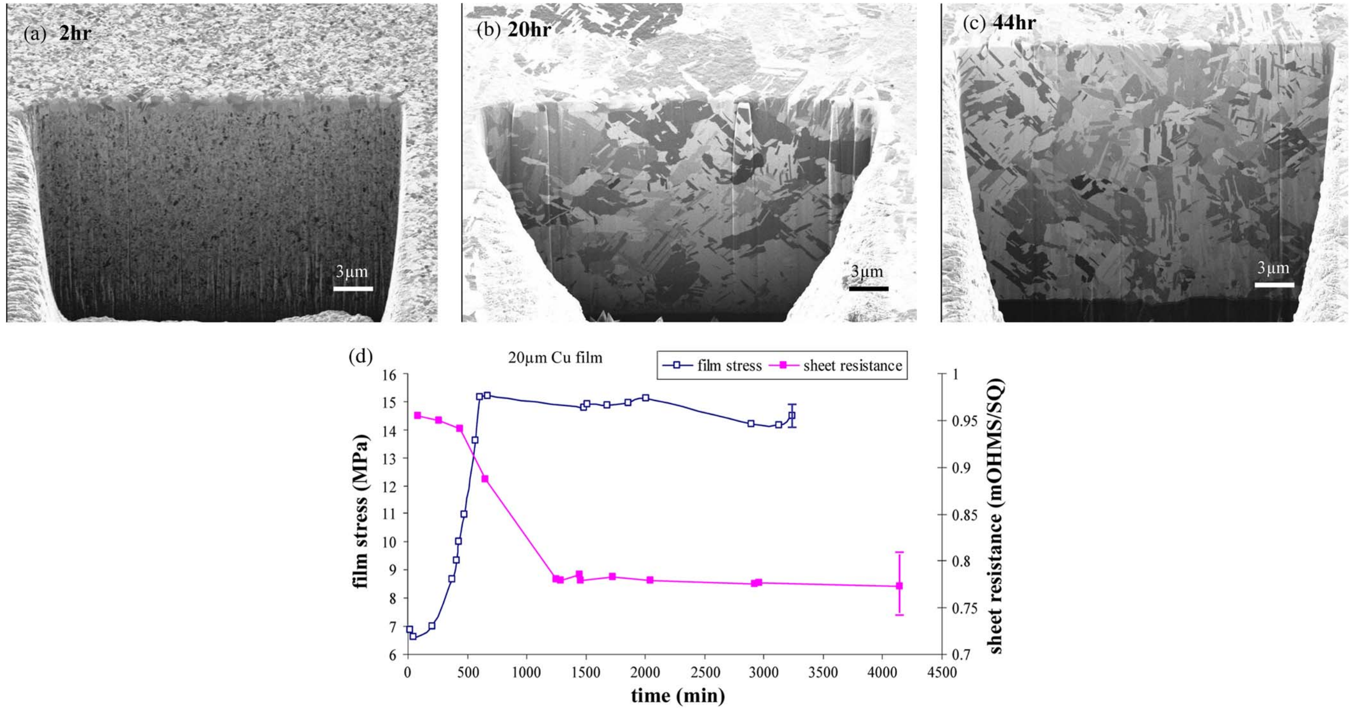

Fig. 3. (a), (b), and (c) 20-μm-thick Cu film grain growth, similar to Figs. 1 and 2. (d) This is also reflected in the decrease of sheet resistance. Again, note an increase in stress like for the 8-μm Cu film in Fig. 2.

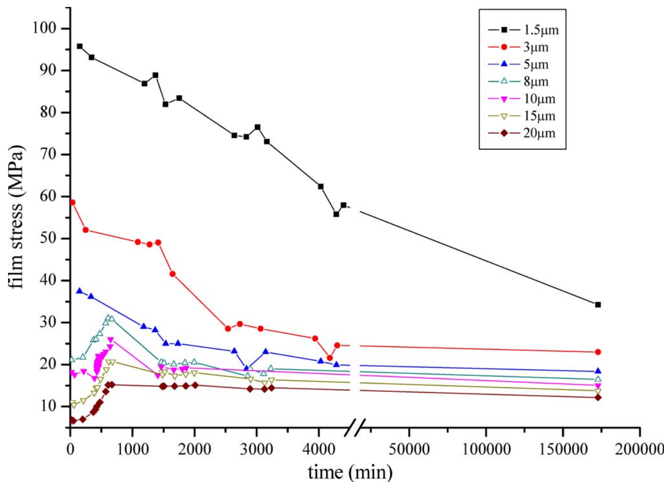

Fig. 4. Film-stress evolution of ECD Cu films (1.5–20 μm). The stresses of 1.5–5-μm-thick Cu films continuously decrease. The stresses of 8–20-μm-thick Cu films have a short incubation period after deposition, before starting to build up tensile stresses. After ∼700 min, the stress decreases. Note, that the film stress measured after four months scales with film thickness.

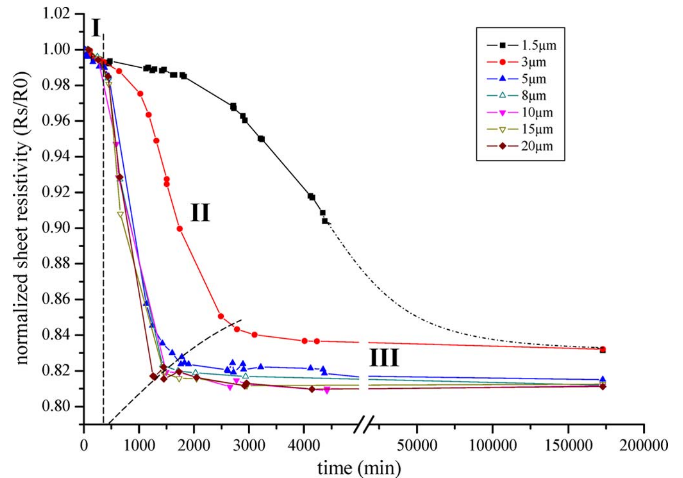

Fig. 5. Sheet-resistance evolution of ECD Cu films (1.5–20 μm). The dash-pointed line for the 1.5-μm-thick Cu film connects the data points of ∼4500 min and approximately four months. (I) Incubation phase. (II) Transient phase. (III) Stagnation phase. During the incubation phase, a small drop ($< 1\%$) of the sheet resistance for all Cu films can be observed. The transient time depends on the film thickness. For the 1.5-μm-thick Cu film, no stabilization is achieved within 4500 min. The sheet resistance has been measured again after a four-month time, indicating a stagnation of the normalized sheet resistance.

IV. Discussion

The discussion is divided into two sections, focusing first on the stress evolution. Second, the decay in sheet resistance is discussed, taking into account the mechanics causing the stress changes with time.

A. Stress Evolution

Two different film-thickness regimes are identified from the stress–time curves. Therefore, both regimes will be discussed, and possible mechanisms for the different behaviors will be proposed.

The continuous decrease of the stress of thin Cu films (1.5–5 μm) in Fig. 4 cannot be directly explained by grain growth. It is speculated that dislocation plasticity causes the stress decrease, as outlined hereafter. As the initial stress is relatively high for thin Cu films, dislocation glide can be activated immediately after deposition and becomes increasingly easier due to grain growth. The stress decrease terminates when the flow stress of the final microstructure, which is film thickness dependent, has been reached. The stress evolution of thick Cu films

Authorized licensed use limited to: Universitatsbibliothek der TU Wien. Downloaded on April 26,2010 at 13:49:58 UTC from IEEE Xplore. Restrictions apply.

(8–20 μm) is more complex. As the initial stress is relatively low and the grain size is small, dislocation glide cannot be activated immediately after deposition. This correlates well to the FIB images in Figs. 2 and 3, which imply that there are no distinct microstructure changes during the first 120 min after deposition. Then, grain growth starts causing a stress increase after the ~200-min incubation phase for the 8–20-μm-thick ECD Cu films. Grain growth leads to annihilation of excess volume by reducing the amount of grain boundaries which induces shrinkage of the film. This gives rise to the tensile stress if the film remains bonded to the substrate. As shown in the FIB images in Figs. 1–3, grain growth clearly occurs during self-annealing. The coarsening starts with the growth of a few grains which consume the surrounding fine-grained matrix until the large grains meet and the fine-grained matrix is completely consumed. Along with grain growth, the tensile film stress increases until it becomes high enough to activate plasticity yielding. As a consequence, both grain growth and plasticity superimpose in the stress evolution. The global stress decreases when the effect of dislocation plasticity becomes more prominent than that of grain growth. This is the case for 8- and 10-μm-thick Cu films (Fig. 4). For the 15- and 20-μm-thick films, the peak stresses are so low that dislocation glide and grain growth counterbalance each other. One should be aware that grain growth also happens for the 1.5–5-μm-thick Cu films. However, no stress increase is observed during room temperature annealing since the initial stress is so high that relaxation by dislocation plasticity is more prominent than the stress increase induced by grain growth.

Figs. 6 and 7 show these processes. The ECD as-deposited films are defect rich due to the low deposition temperature process and Cl, S, and C impurities [14] coming from the electrolyte bath. The incubation time may be caused by the segregation of impurities via the grain boundaries to the film surface and/or film/substrate interface, as shown in Fig. 6(a) and (b). Then, Ostwald ripening [9], [28] can set in with grain growth starting at grains where grain boundaries are released first by surface and interface segregation of impurities [Fig. 6(a)–(c)]. It implies that the stress itself is not the only driving force for self-annealing. Otherwise, the thicker film would not anneal so rapidly. The driving force for room temperature grain growth originates from the minimization of the total energy of the system. A large variety of energies, such as strain energy, grain boundary energy, surface/interface energy, dislocation energy, and stacking-fault energy are assumed in the literature to be involved in this process [9], [11], [13], [18], [22], [28]. The existence of a high density of defects, mostly impurities, dislocations, and grain boundaries introduced by room-temperature ECD, is considered as the main source of a large amount of energy stored in the as-deposited fine grains of electroplated Cu films [11], [18], [22].

However, as aforementioned, the grain growth of a thin film on a substrate leads to a stress increase due to elimination of excess volume following the relationship summarized by Nix [25]:

$$\sigma_{\mathrm{gg}} = \frac{E}{1-\upsilon} 2\Delta \mathrm{a} \left(\frac{1}{d_0} - \frac{1}{d}\right) \tag{2}$$

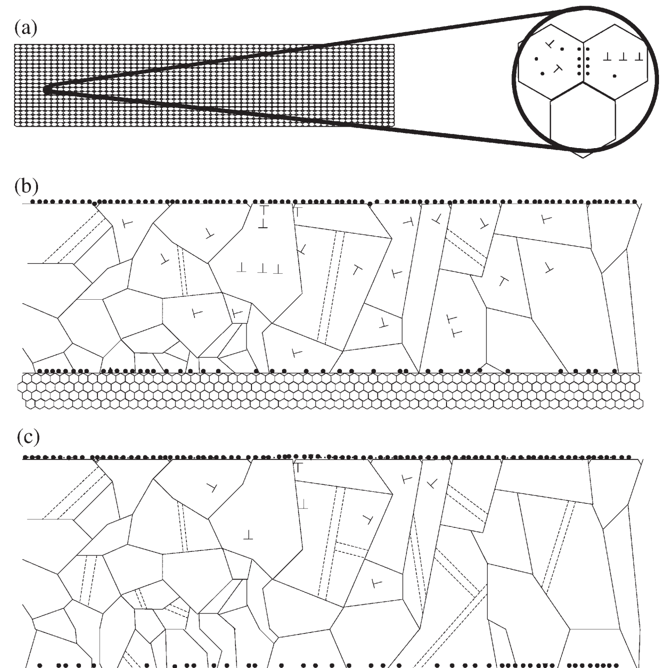

Fig. 6. Illustration of the microstructure evolution. Dashed lines indicate twins. (a) Only fine grains exist in the film after deposition, coupled with a high density of impurities and dislocations. Impurities pin at the grain boundaries. (b) Impurities segregate to the film surface and/or film/substrate interface, thus releasing the grain boundaries. Grain growth starts and finally reaches the film/substrate interface region. Meanwhile, dislocation glide can be activated. (c) Grain growth terminates. Dislocation density is reduced because dislocations glide across the grains and are incorporated into the grain boundaries.

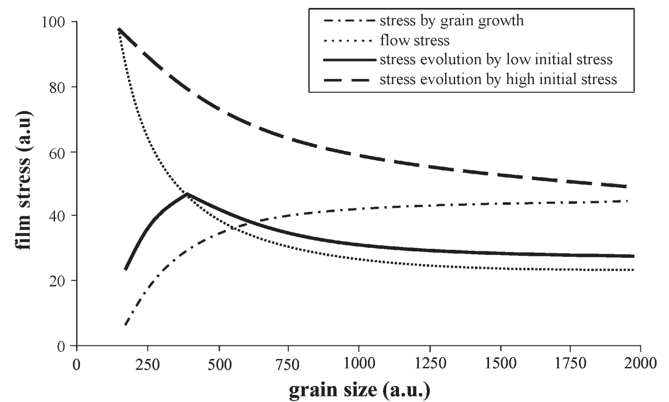

Fig. 7. Film-stress evolution curves with grain size shown, assuming a stress increase proportional to $1/d$ for grain growth and a grain-size-dependent flow stress with $\sigma \sim 1/\sqrt{d}$. When the initial stress is high, it allows dislocation plasticity throughout grain growth. When the initial stress is low, it permits dislocation plasticity only above a critical grain size.

where σ_{gg} is the film-stress increase induced by grain growth, E is the elastic modulus of the film, υ is the Poisson's ratio of the film, Δa is the excess volume per unit area of grain boundary, d_0 is the as-deposited grain size, and d is the final grain size. This model calculates the intrinsic stress associated with grain growth, assuming spherical grains involved in the film.

In contrast, the dislocation glide of deposition-induced dislocations relaxes the stress. In order to activate dislocation plasticity, the film stress must exceed the flow stress which

Authorized licensed use limited to: Universitatsbibliothek der TU Wien. Downloaded on April 26,2010 at 13:49:58 UTC from IEEE Xplore. Restrictions apply.

scales for polycrystalline Cu films with grain size, following the Hall–Petch relation [29]

$$\sigma_{\mathrm{HP}} = \sigma_0 + \frac{K}{\sqrt{d}} \tag{3}$$

where σ_{HP} is the film stress, σ_0 is the friction stress, K is the Hall–Petch coefficient, and d is the grain size.

Using Nix's grain-growth model and the Hall–Petch law, one can plot flow stress as a function of grain-size evolution, as shown in Fig. 7. With the assumption that grains grow from 140 nm to 2 μm, the increasing grain size decreases the flow stress in a film of constant film thickness.

In our case, both models, grain growth and grain-size-dependent dislocation plasticity, superimpose, as shown in Fig. 7, where two different initial stresses are assumed: a high stress in the as-deposited state and a low as-deposited stress. The as-deposited stress determines the further development of film stress. If the as-deposited stress is relatively high, the total stress relaxes due to dislocation glide. In contrast, if the as-deposited stress is relatively low, grain growth will enhance the total film stress until the yield stress is reached, and then, plasticity relaxes the stress level.

We believe that, for thinner films, due to the shorter total deposition time, a higher defect density evolves, leading to the higher initial stress compared to thicker films where some of the defects already annihilate during the longer deposition time. This could explain why the initial stress decreases with increasing film thickness (i.e., deposition time). Moreover, the "zipping" process of grain boundaries could be also responsible for the film-thickness dependence of the initial stress [30]. It can be speculated that the grain size increases slightly with deposition thickness, leading to lower initial film stresses by grain boundary "stretching" for thicker films. However, due to the resolution limit of FIB imaging (~50 nm in our case), the possible grain-size difference for different film thicknesses could not be resolved. The grain-size evolution starts with a small volume fraction of grains which grow with time, while other grains start to grow at a later stage. This leads to a bimodal grain-size distribution (see Fig. 8). As a consequence, a simple addition of (2) and (3) does not suffice to predict the final stress values, but provides a guideline to explain the observed stress evolutions in Fig. 4. Further modeling activities are required to obtain a quantitative description.

B. Sheet-Resistance Evolution

The sheet resistance is determined by the scattering of electrons at defects in the film such as impurities, dislocations, and grain boundaries. The annihilation of defects reduces the sheet resistance. Similarly as for the stress evolution, different regimes are observed and can be explained by the same mechanisms as for the stress evolution. During the first ~400 min, the sheet resistance decreases slightly (<~1%), because impurity scattering is reduced by the diffusion and coalescence of impurities at grain boundaries [see Fig. 6(a)]. The segregation of the impurities to the surface and interface unpins the grain boundaries, leading to grain growth [see Fig. 6(b)] correlating well to regime II in Fig. 5 which shows a dramatic decrease of normalized sheet resistance caused by the loss of electron scattering sources (i.e., grain boundaries). During this transient regime, a size effect is observed. The transient time depends on the film thickness and increases in time for thinner films. This becomes particularly obvious for the 1.5- and 3-μm-thick Cu films while, for the 5–20-μm-thick Cu films, the transient time is rather constant. Comparing the evolution of the sheet resistance in Fig. 5 with the film-stress evolution in Fig. 4 and the microstructure investigations in Figs. 1–3, it can be concluded that regime II depends on grain growth (annihilation of grain boundaries) and dislocation plasticity (decreasing dislocation density due to the stress evolution and stress relaxation). It is well known that ECD Cu can initially have a high dislocation density $(10^{12} - 10^{13}\ \mathrm{cm}^{-2})$ [28], which will decrease by annihilation at grain boundaries during yielding and grain growth. Finally, the sheet resistance stagnates in regime III where grain growth and stress relaxation have terminated. This demonstrates that grain growth and dislocation glide not only affect the stress evolution during room temperature annealing but are also reflected in the sheet-resistance evolution.

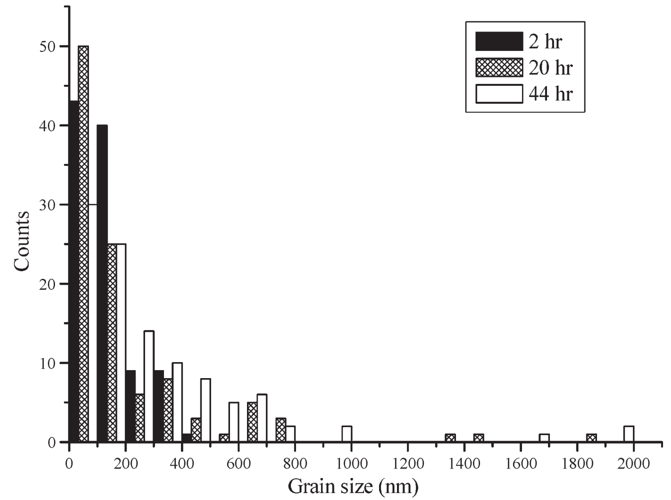

Fig. 8. Grain-size distribution of a 3-μm ECD Cu film during grain growth. The data are deduced from FIB images with the linear intercept method. A bimodal grain-size distribution is observed after grain growth starts.

V. Summary and Conclusion

New insights have been gained in the stress and sheet-resistance evolution during self-annealing of ECD Cu by studying film thicknesses between 1.5 and 20 μm. The main findings are as follows.

1) In the first ~500 min after deposition, the film stress (except 1.5–5-μm-thick films) and sheet resistance remain rather constant. This is explained by the segregation of impurities toward the grain boundaries.
2) Grain growth is observed by FIB studies. This is explained by the segregation of impurities toward the film surface and interface, unpinning the grain boundaries.
3) Grain growth leads to a decrease in sheet resistance. For thick films, the low as-deposited tensile stress increases due to the annihilation of excess volume, while for thin films due to the already preexisting high as-deposited

Authorized licensed use limited to: Universitatsbibliothek der TU Wien. Downloaded on April 26,2010 at 13:49:58 UTC from IEEE Xplore. Restrictions apply.

tensile stress, grain growth induces yielding and, thus, a reduction in film stress.

4) Finally, grain growth terminates, and stress relaxation by dislocation glide is exhausted. The film stress and sheet resistance stagnate at a certain value which scales with film thickness.

This paper reveals that the stress and sheet-resistance evolution after the deposition of electroplated copper films can be explained by grain growth and grain-size-dependent yielding. However, quantitative modeling is complex due to the inhomogenous microstructure evolution and will remain a challenging task. For applications of ECD Cu in devices, thicker films are technologically more suitable since (meta)stable conditions are reached after shorter time periods during room-temperature annealing, while thinner films reveal substantial changes in stress and sheet resistance over longer time periods.

ACKNOWLEDGMENT

The authors would like to thank M. Kirchberger for the FIB measurements and M. Schneegans and P. Nelle for the helpful discussions.

REFERENCES

[1] C. K. Hu, B. Luther, F. B. Kaufman, J. Hummel, C. Uzoh, and D. J. Pearson, "Copper interconnection integration and reliability," *Thin Solid Films*, vol. 262, no. 1/2, pp. 84–92, Jun. 1995.

[2] M. D. Thouless, J. Gupta, and J. M. E. Harper, "Stress development and relaxation in copper-films during thermal cycling," *J. Mater. Res.*, vol. 8, no. 8, pp. 1845–1852, Aug. 1993.

[3] D. Edelstein, J. Heidenreich, R. Goldblatt, W. Cote, C. Uzoh, N. Lustig, P. Roper, T. McDevitt, W. Motsiff, and A. Simon, "Full copper wiring in a sub-0.25 μm CMOS ULSI technology," in *IEDM Tech. Dig.*, 1997, pp. 773–776.

[4] L. T. Romankiw, "A path: From electroplating through lithographic masks in electronics to LIGA in MEMS," *Electrochim. Acta*, vol. 42, no. 20–22, pp. 2985–3005, 1997.

[5] P. C. Andricacos, C. Uzoh, J. O. Dukovic, J. Horkans, and H. Deligianni, "Damascene copper electroplating for chip interconnections," *IBM J. Res. Develop.*, vol. 42, no. 5, pp. 567–574, Sep. 1998.

[6] K. Pantleon and M. A. J. Somers, "In situ investigation of the microstructure evolution in nanocrystalline copper electrodeposits at room temperature," *J. Appl. Phys.*, vol. 100, no. 11, p. 114 319, Dec. 2006.

[7] C. Lingk and M. E. Gross, "Recrystallization kinetics of electroplated Cu in damascene trenches at room temperature," *J. Appl. Phys.*, vol. 84, no. 10, pp. 5547–5553, Nov. 1998.

[8] S. H. Brongersma, E. Richard, I. Vervoort, H. Bender, W. Vandervorst, S. Lagrange, G. Beyer, and K. Maex, "Two-step room temperature grain growth in electroplated copper," *J. Appl. Phys.*, vol. 86, no. 7, pp. 3642–3645, Oct. 1999.

[9] J. M. E. Harper, C. Cabral, Jr., P. C. Andricacos, L. Gignac, I. C. Noyan, K. P. Rodbell, and C. K. Hu, "Mechanisms for microstructure evolution in electroplated copper thin films near room temperature," *J. Appl. Phys.*, vol. 86, no. 5, pp. 2516–2626, Sep. 1999.

[10] W. Wu, D. Ernur, S. H. Brongersma, M. Van Hove, and K. Maex, "Grain growth in copper interconnect lines," *Microelectron. Eng.*, vol. 76, no. 1–4, pp. 190–194, Oct. 2004.

[11] V. Weihnacht and W. Brückner, "Abnormal grain growth in {111} textured Cu thin films," *J. Appl. Phys.*, vol. 418, no. 2, pp. 136–144, Oct. 2002.

[12] C. H. Seah, G. Z. You, C. Y. Li, and R. Kumar, "Characterization of electroplated copper films for three-dimensional advanced packaging," *J. Vac. Sci. Technol. B, Microelectron. Nanometer Struct.*, vol. 22, no. 3, pp. 1108–1113, May/Jun. 2004.

[13] S. P. Hau-Riege and C. V. Thompson, "In situ transmission electron microscope studies of the kinetics of abnormal grain growth in electroplated copper films," *Appl. Phys. Lett.*, vol. 76, no. 3, pp. 309–311, Jan. 2000.

[14] M. Stangl, M. Lipták, A. Fletcher, J. Acker, J. Thomas, H. Wendrock, S. Oswald, and K. Wetzig, "Influence of initial microstructure and impurities on Cu room-temperature recrystallization (self-annealing)," *Microelectron. Eng.*, vol. 85, no. 3, pp. 534–541, Mar. 2008.

[15] M. T. Pérez-Prado and J. J. Vlassak, "Microstructural evolution in electroplated Cu thin films," *Scr. Mater.*, vol. 47, no. 12, pp. 817–823, Dec. 2002.

[16] Q. T. Jiang and M. E. Thomas, "Recrystallization effects in Cu electrodeposits used in fine line damascene structures," *J. Vac. Sci. Technol. B, Microelectron. Nanometer Struct.*, vol. 19, no. 3, pp. 762–766, May 2001.

[17] D. Kwon, H. Park, S. Ghosh, C. M. Lee, H. T. Jeon, and J. G. Lee, "Recrystallization of the copper films deposited by pulsed electroplating on ECR plasma-cleaned copper seed layers," *J. Korean Phys. Soc.*, vol. 44, no. 5, pp. 1108–1112, May 2004.

[18] S. Lagrange, H. Brongersma, M. Judelewicz, A. Saerens, I. Vervoort, E. Richard, R. Palmans, and K. Maex, "Self-annealing characterization of electroplated copper films," *Microelectron. Eng.*, vol. 50, no. 1, pp. 449–457, Jan. 2000.

[19] W. H. Teh, L. T. Koh, S. M. Chen, J. Xie, C. Y. Li, and P. D. Foo, "Study of microstructure and resistivity evolution for electroplated copper films at near-room temperature," *Microelectron. J.*, vol. 32, no. 7, pp. 579–585, Jul. 2001.

[20] K. B. Yin, Y. D. Xia, C. Y. Chan, W. Q. Zhang, Q. J. Wang, X. N. Zhao, A. D. Li, Z. G. Liu, M. W. Bayes, and K. W. Yee, "The kinetics and mechanism of room-temperature microstructural evolution in electroplated copper foils," *Scr. Mater.*, vol. 58, no. 1, pp. 65–68, Jan. 2008.

[21] K. B. Yin, Y. D. Xia, W. Q. Zhang, Q. J. Wang, X. N. Zhao, A. D. Li, Z. G. Liu, X. P. Hao, L. Wei, C. Y. Chan, K. L. Cheung, M. W. Bayes, and K. W. Yee, "Room-temperature microstructural evolution of electroplated Cu studied by focused ion beam and positron annihilation lifetime spectroscopy," *J. Appl. Phys.*, vol. 103, no. 6, pp. 066 103-1–066 103-3, 2008.

[22] H. Lee, W. D. Nix, and S. S. Wong, "Studies of the driving force for room-temperature microstructure evolution in electroplated copper films," *J. Vac. Sci. Technol. B, Microelectron. Nanometer Struct.*, vol. 22, no. 5, pp. 2369–2374, Sep./Oct. 2004.

[23] V. A. Vas'ko, I. Tabakovic, S. C. Riemer, and M. T. Kief, "Effect of organic additives on structure, resistivity, and room-temperature recrystallization of electrodeposited copper," *Microelectron. Eng.*, vol. 75, no. 1, pp. 71–77, Jul. 2004.

[24] W. Robl, M. Melzl, B. Weidgans, R. Hofmann, and M. Stecher, "Last metal copper metallization for power devices," *IEEE Trans. Semicond. Manuf.*, vol. 21, no. 3, pp. 358–362, Aug. 2008.

[25] M. F. Doerner and W. D. Nix, "Stresses and deformation processes in thin films on substrates," *Crit. Rev. Solid State Mater. Sci.*, vol. 14, no. 3, pp. 225–268, 1988.

[26] L. B. Freund and S. Suresh, *Thin Film Materials: Stress, Defect Formation, and Surface Evolution*. Cambridge, U.K.: Cambridge Univ. Press, 2003.

[27] W. D. Nix, "Mechanical properties of thin films," *Metall. Trans. A*, vol. 20, pp. 2217–2245, 1989.

[28] C. Detavernier, S. Rossnagel, C. Noyan, S. Guha, C. Cabral, and C. Lavoie, "Thermodynamics and kinetics of room-temperature microstructural evolution in copper films," *J. Appl. Phys.*, vol. 94, no. 5, pp. 2874–2881, Sep. 2003.

[29] T. H. Courtney and T. Hugh, *Mechanical Behavior of Materials*. New York: McGraw-Hill, 1990.

[30] B. W. Sheldon, A. Rajamani, A. Bhandari, E. Chason, S. K. Hong, and R. Beresford, "Competition between tensile and compressive stress mechanisms during Volmer–Weber growth of aluminum nitride films," *J. Appl. Phys.*, vol. 98, no. 4, pp. 043 509-1–043 509-9, Aug. 2005.

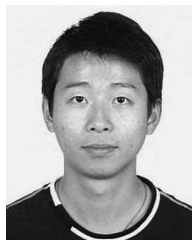

Rui Huang received the B.S. degree in materials science and engineering from Zhejiang University, Zhejiang, China, and the M.S. degree in materials science and engineering from Kiel University, Kiel, Germany. He is currently working toward the Ph.D. degree with Kompetenzzentrum Automobil- und Industrieelektronik GmbH (KAI), Villach, Austria, in cooperation with the institute of Microelectronics, Technische Universität Wien (TU Vienna), Vienna, Austria.

His research is focused on mechanical and thermomechanical properties of copper metallization used in semiconductor devices.

Authorized licensed use limited to: Universitatsbibliothek der TU Wien. Downloaded on April 26,2010 at 13:49:58 UTC from IEEE Xplore. Restrictions apply.

Werner Robl received the Ph.D. degree in physics from the University of Regensburg, Regensburg, Germany, in 1994.

Then, he joined Infineon Technologies (formerly Siemens Semiconductors), Regensburg, where he has been working on development of new metallization schemes in Regensburg and Munich, Germany, and East Fishkill, NY, and is currently a Principal for Metallization on new metallization schemes for semiconductor devices and chip packaging.

Dr. Robl is a member of the German Physical Society.

Hajdin Ceric was born in Sarajevo, Bosnia and Herzegovina, in 1970. He studied electrical engineering with the University of Sarajevo, Sarajevo, and received the Dipl.Ing. degree in 2000 and the Ph.D. degree in technical sciences in 2005 from Technische Universität Wien, Vienna, Austria.

In June 2000, he joined the Institute for Microelectronics, Technische Universität Wien, where he is currently a Postdoctoral Researcher. His scientific interests include interconnect and process simulation.

Thomas Detzel received the M.S. degree in physics from the University of Konstanz, Konstanz, Germany, and the Ph.D. degree in surface and thin-film physics in 1994 from the Max-Planck-Institute, Garching, Germany. He studied his junior year at Rutgers University, New Brunswick, NJ.

He was a Postdoc with the Institut de Physique et Chimie des Matériaux de Strasbourg, Strasbourg, France. In 1995, he was with Rodel Europe GmbH, where he was an Application Manager for chemical–mechanical polishing. In 1999, he joined Infineon Technologies Austria AG, Villach, Austria, where he was responsible for the metallization development of power semiconductors, has been the Project Manager of different power integrated circuit developments since 2004, and has been leading the research project Robust Metallization and Interconnect in the Competence Center for Automotive and Industrial Electronics since 2006.

Dr. Detzel is an alumnus of the German National Academic Foundation and a member of the German Physical Society.

Gerhard Dehm received the M.S. degree in materials science from the University of Erlangen-Nürnberg, Erlangen, Germany, and the Ph.D. degree from the University of Stuttgart, Stuttgart, Germany.

He spent about 10 years with the Max Planck Institute of Metals Research, Stuttgart, before moving in 2005 to Austria. In addition, he was a Guest Scientist with the Technion-Israel Institute of Technology, Haifa, Israel, for two years. He is currently the Head of the Department of Materials Physics, Montanuniversität Leoben, Leoben, Austria. He is also the Director of the Erich Schmid Institute of Materials Science, Austrian Academy of Sciences, Leoben. He is the author of more than 160 scientific publications.

Prof. Dehm is a recipient of scientific awards from the German Society of Materials Science (DGM) and the award for Nanosciences and Nanotechnology from Styria (Austria).

Authorized licensed use limited to: Universitatsbibliothek der TU Wien. Downloaded on April 26,2010 at 13:49:58 UTC from IEEE Xplore. Restrictions apply.